Int. J. Electrochem. Sci., 12 **(2017)** 11506 – 11514, doi: 10.20964/2017.12.67

International Journal of
ELECTROCHEMICAL
SCIENCE
www.electrochemsci.org

Combined Determination of Carbohydrate Antigen 199 and SirT1 Based on an Electrochemiluminescence Immunosensor

Wei Shao[1], *Xiuli Sui*[2] *and Guowei Wang*[3,*]

[1] Department of Neurosurgery, Binzhou Medical University Hospital, Binzhou City, Shandong Province, 256603, P.R. China
[2] Clinical laboratory, WenDeng Osteopathy Hospital, WeiHai City, Shandong Province, 250012, P.R. China
[3] Department of Neurosurgery, The First Hospital of Yulin, Yulin City, Shaanxi Province, 719000, P.R. China
[*]E-mail: weishaoneuro@yeah.net

Received: 18 August 2017 / *Accepted:* 13 October 2017 / *Published:* 12 November 2017

In this work, a multi-functionalized graphene oxide (GO) material, where N-(4-aminobutyl)-N-ethylisoluminol (ABEI) and either a CA199 antibody or a SirT1 antibody were chemically bound to the surface of magnetic GO (nanoFe_3O_4@GO), was fabricated as a one-step electrochemiluminescence (ECL) immunosensor for the ultrasensitive determination of the carbohydrate antigen 199 (CA199) and human sirtuin1 (SirT1). The determination was carried out using a sandwich system, with the quantification of CA199 and SirT1 achieved through potential cycling from +0.6 to −1.4 V. This strategy was successfully used for the determination of the two tumour markers over the range of 0.3 fg/mL - 22 pg/mL, and the limit of detection (LOD) was calculated as 0.15 fg/mL.

Keywords: Combined determination; Carbohydrate antigen 199; Electrochemiluminescence method; Glioma diagnosis;

1. INTRODUCTION

The effect of sirtuins on the lifespan of yeast led to extensive focus on their role in age-related diseases and prolonging a calorie restriction (CR)-dependent lifespan [1, 2]. As one of the main sirtuins, human sirtuin1 (SirT1) has been reported to regulate the influence of calorie restriction (CR) on lifetime, and evidence has shown that it may control and regulate some pathways for the CR-mediated metabolic feedback [3]. The upregulation of SirT1 has been confirmed to pose an essential protective effect against a large number of diseases in animal models, based on substantial reports [4].

In addition, the overexpression of SirT1 has been found to prolong the lifespan of diverse organisms, while SirT1 deletion or mutations have been confirmed to decrease lifespan [5]. To facilitate the understanding of the contribution of SirT1 to both a long lifespan and CR-mediated lifespan extension, it is necessary to develop a sensitive and accurate analytical method for the detection of SirT1 [6, 7]. Carbohydrate antigen-199 (CA199) and SirT1 have been confirmed to be related to glioma and pancreatic tumours. Furthermore, the majority of cancers show high levels of at least two TMs related to their incidence. These results suggested the necessity of simultaneous detection of multiple TMs in clinical laboratories [8].

Currently, the primary techniques applied to the detection of cancer markers include a radioimmunoassay [9-11], electrochemical immunoassay [12-14], chemiluminescence immunoassay [15-17] and enzyme-linked immunoabsorbent assay [18-20]. Nevertheless, their practical use also suffers many disadvantages, including prolonged detection time, the necessity of toxic or radioactive markers, and sophisticated experimental procedures. To solve these constraints for better performance, specialized lab-chips and lateral flow apparati have been reported, providing within-minutes assays [21-23], microlitre consumption of samples, and adequately sensitive determination of clinically relevant biomarker targets. Furthermore, some of them are characteristic of reduced sophistication, along with being low-cost and requiring portable ancillary instrumentation in clinical cases [24, 25]. However, improvement in the determination sensitivity remains essential, due to the relatively low concentration of some biomarker targets in urine and saliva compared with that of the serum, esp. in the case of inadequate sample quantities. Hence, it is still necessary to develop a reliable, sensitive, and facile strategy for the determination of CA19-9 and other low abundance tumour markers, particularly for use in clinical diagnostics.

As a layered compound, graphene oxide (GO) can be synthesized through the oxidation of natural graphite. The formation of nanoFe_3O_4@GO through the easy loading of magnetic iron oxide nanoparticles onto GO that contains oxygenated functional groups, including 6-membered lactol rings, ketones, carboxyl groups, hydroxyl groups and epoxides; desirable electrical conductivity; and large surface area [26] could be promising for use in diverse fields, including environmental remediation, catalysis, magnetic fluids, magnetic energy storage, and biomedicine [27]. Furthermore, multi-functionalized GO materials, where nanoFe_3O_4@GO is further functionalized with aptamers, DNAs, enzymes, antibodies, and/or diverse labels, etc. have gained substantial attention [28]. Nevertheless, the application of multi-functionalized GO in the fabrication of immunosensors has been rarely reported.

Electrochemiluminescence (ECL) is highly sensitive, has a simplified optical setup, and possesses exceptionally low background signal and a wide dynamic range and thus exhibits excellent performance for the preparation of immunosensors. Additionally, N-(4-aminobutyl)-N-ethylisoluminol (ABEI), a derivative of luminal and a desirable immunoassay marker due to its amino group, is one of the most extensively applied systems [29]. The ECL immunoassay shows remarkable selectivity, sensitivity, rapidness, simplified optical setup, and requires only a short assay time for the determination of disease-related proteins; these advantages are ascribed to the synergistic effect of ECL and specific recognition of immunoassay [30].

This work proposes the fabrication of a multi-functionalized GO through the chemical binding of an antibody to the nanoFe_3O_4@GO surface to achieve a one-step ECL immunosensor for the ultrasensitive determination of CA199 and SirT1. This immunosensor provides exceptionally sensitive, stable, specific, and simple determination. Therefore, our developed strategy has the potential to be used for the determination of tumour markers in glioma diagnostics.

2. EXPERIMENTS

2.1. Chemicals

N-hydroxysuccinimide (NHS), 1-ethyl-3-(3-dimethylaminopropyl) carbodiimide hydrochloride (EDC), N-(4-aminobutyl)-N-ethylisoluminol (ABEI), and bovine serum albumin (BSA) were commercially available in Sigma-Aldrich (St. Louis, MO, USA). Carbohydrate antigen 19-9 (CA199), CA199 antibody (anti-CA199), antigen SirT1 and antibody SirT1 were commercially available from Shanghai Linc-Bio Science Co., Ltd. (Shanghai, China). 25% NH_4OH (wt%), 30% H_2O_2 (wt%), $FeCl_2{\cdot}4H_2O$, and ferric chloride hexahydrate ($FeCl_3{\cdot}6H_2O$) were commercially available from Sinopharm Chemical Reagent Co., Ltd. (Shanghai, China). To prepare carbonate buffer solution (CBS), $NaHCO_3$ was mixed with $Na_2CO_3{\cdot}10H_2O$, with the pH adjusted to 9.90 unless otherwise stated. Ultrapure water was provided by a Millipore water purification system (≥18 MΩ) and was used in all the experiments. All other chemicals were of analytical reagent grade and were used without additional purification.

2.2. Apparatus

All electrochemical measurements for the ECL were carried out at ambient temperature in a conventional three-electrode configuration using Autolab electrochemical analyser model PGSTAT30 (Eco Chemie, Utrecht, The Netherlands), a potentiostat linked to GPES software (Eco Chemie). ECL experiments were performed using a homemade analyser. A bare magnetic glassy carbon electrode (GCE) was purchased from Yidian Technology Co. Ltd. This three-electrode configuration consisted of a modified magnetic GCE working electrode, Ag/AgCl reference electrode, and a platinum wire counter electrode. Electrochemical impedance spectroscopy (EIS) experiments were carried out in 0.1 M KCl solution with 5 mM $Fe(CN)_6^{3-/4-}$, using a ZAHNER (model IM6ex, Germany) involved electrochemical system, where the experimental data were fitted using Z value software. The SirT1 and CA199 concentration related ECL signals were recorded by assembling the as-prepared sandwich-type immunosensors (50 μL) with varying SirR1 and CA199 concentrations onto the GCE surface through a magnet. This was followed by adding ten millilitres of phosphate buffer (0.1 M, pH 7.4) and 12 mM H_2O_2 to the detector cell and scanning the as-prepared electrode over a range of 0.6 V to −1.4 V (scan rate, 100 mV/s). Finally, the SirT1 (600 nm) and CA199 (425 nm) concentration related ECL signals were obtained after placing the emission window in front of the PMT at 800 V via placing two band pass filters.

2.3. Synthesis of magnetic nanoFe_3O_4@GO

Hummer's method was used for the preparation of graphene oxide (GO). Conventionally, Fe_3O_4@GO was prepared by dispersing GO (40 mg) in water (40 mL) under 0.5 h ultrasonication in a round-bottom flask, which was subsequently mixed with 50 mL of an iron source solution plus 300 mg of $FeCl_2 \cdot 4H_2O$ and 800 mg of $FeCl_3 \cdot 6H_2O$ and vigorously stirred at ambient temperature. After heating to 85 °C, this mixture was further mixed dropwise with 25% hydroxide (wt%) to increase the pH to 10. After rapid stirring for 45 min, a black composite was obtained as the final product, i.e., magnetic nanoFe_3O_4@GO. After extraction using a magnet, this product was repeatedly washed using water several times.

2.4. Preparation of multi-functionalized GO/anti-CA199 (or anti-SirT1)/ABEI–nanoFe_3O_4@GO composite

A mixed solution of NHS (10 mg/mL) and EDC (100 mg/mL) was further mixed with the as-prepared nanoFe_3O_4@GO (200 µL, 1 mg/mL), and the pH was adjusted to 5. A stable active ester layer was formed on GO surface after shaking this mixture for 60 min at room temperature. A magnet was used for a thorough washing of the final black precipitate 3 times. After adding 100 µL of the mixture of either anti-SirT1 or anti-CA199 (0.5 ng/mL) and ABEI (13.8 µg/mL), the obtained mixed solution was shaken for an additional 4 h. After the addition of BSA (100 µL, 2 wt%), a final black composite was yielded, which was left reacting for 60 min to block non-specific binding sites. After washing and reconstructing in water (200 µL), the final product was yielded, i.e., the multi-functionalized anti-CA199 (SirT1)/ABEI–nanoFe_3O_4@GO composite. Herein, the recognition and capture of the target CA199 was achieved by anti-CA199 (SirT1), while the electrochemiluminophore was captured by SirT1. Additionally, the one-step construction of the ECL immunosensor was achieved due to nanoFe_3O_4, as well as the above compounds.

3. RESULTS AND DISCUSSION

The main aim of the present investigation was to determine biomarkers, so the performance of the prepared biosensor was assessed by detecting standard solutions with the ECL technique. For both the bare magnetic GCE and nanoFe_3O_4@GO modified electrode, there were no ECL signals recorded, as shown in Figure 1A. However, a considerable ECL response was recorded on the ABEI–nanoFe_3O_4@GO modified electrode, which suggested the electrochemiluminophore (i.e., ABEI) had been successfully immobilized onto GO. On the other hand, a decrease in ECL intensity was found with the anti-CA199/ABEI–nanoFe_3O_4@GO. This was because the ECL signal emitted from the electrode surface was hindered by the immobilization of BSA and anti-CA199, which also led to the inhibition of the ECL reaction by blocking the charge transport on the electrode interface. The ECL intensity was significantly decreased after incubating the immunosensor in a sample that contained CA199 (0.5 U/mL), which was linked to the electrode surface via an antigen–antibody reaction. These

results illustrated that the cross-reactivity between the two tumour markers was negligible [31, 32]. The explanation for the background signal is the non-specific adsorption caused by the high concentration of the binding buffer on the electrode surface [33].

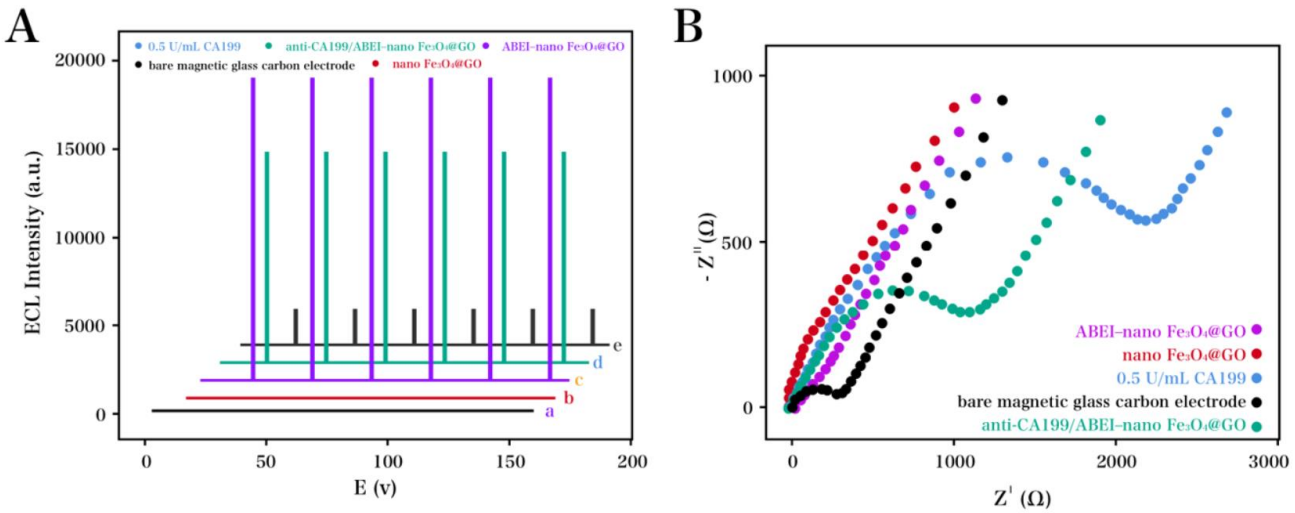

Figure 1. (A) ECL responses recorded using bare magnetic GCE, nanoFe_3O_4@GO, ABEI–nanoFe_3O_4@GO, anti-CA199/ABEI–nano Fe_3O_4@GO, and 0.5 U/mL CA199. (B) EIS profiles of bare magnetic GCE, nanoFe_3O_4@GO, ABEI–nano Fe_3O_4@GO, anti-CA199/ABEI–nanobFe_3O_4@GO, and 0.05 U/mL CA199.

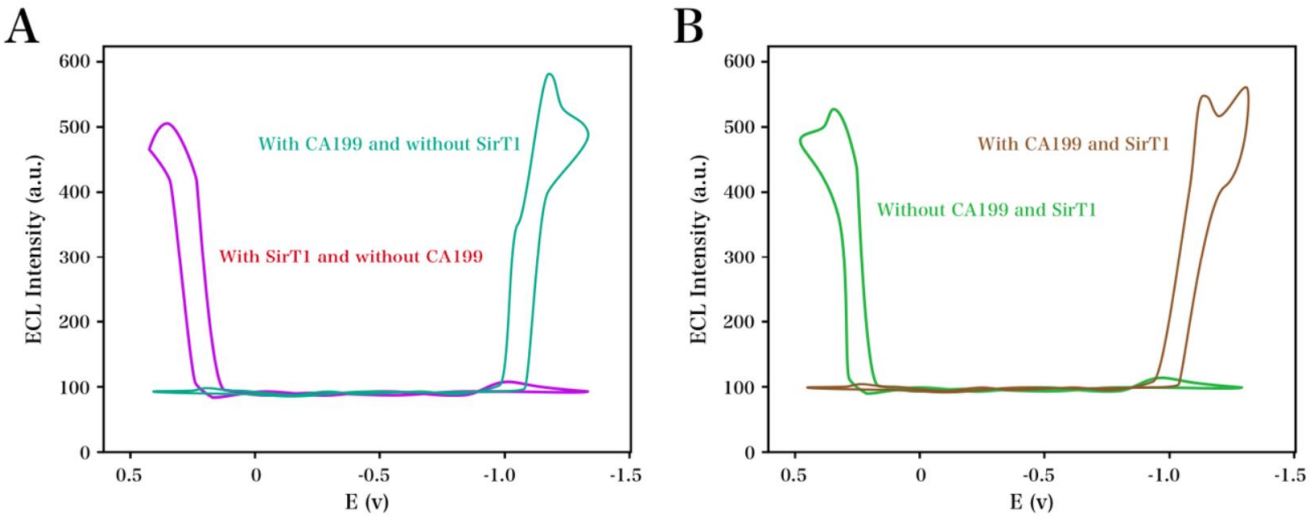

Figure 2. (A) ECL signals recorded with CA199 (without SirT1). (B) ECL signals recorded with SirT1 (without CA199).

For the EIS profile, a semicircle and a line are shown at the high and low AC modulation frequencies, respectively, with the electron transfer resistance (R_{et}) corresponding to the former. In contrast, the linear portion coinciding with the diffusion limited electron shift occurred at comparatively lower frequencies. It can be proposed that the spectra were similar to those of Randle's equivalent circuit in theory [34, 35]. Compared with the bare magnetic GCE, the electrode after modification with nanoFe_3O_4@GO showed a considerable decrease in the semicircle diameter, ascribed to the desirable electrical conductivity of nanoFe_3O_4 and GO, as displayed in Figure 1B. A

slight increase in R_{et} was observed upon the immobilization of ABEI molecules. In contrast, a considerable increase in R_{et} was observed during the construction of the immunosensor, due to the subsequent conjugation and increased difficulty for charge transfer. Another remarkable increase in R_{et} was found when the concentration of CA199 was 0.05 U/mL, since the formation of an insulating protein layer on the assembled surface by antigen immobilization led to further hindrance of the interfacial electron transfer.

As shown in Figure 2A, the cross-reactivity between the two tumour markers was investigated by incubating the immunosensor with a single CA199-containing solution or single SirT1-containing solution. It was found that both anti-CA199/ABEI–nanoFe_3O_4@GO and anti-SirT1/ABEI–nanoFe_3O_4@GO only showed ECL signals in the presence of their corresponding antigens, as expected. As shown in Figure 2B, when CA199 and SirT1 were simultaneously added, an increase in the ECL intensity was observed at specific potentials and wavelengths. In addition, the ECL intensities obtained herein were comparable with those obtained when CA199 or SirT1 were added separately.

The influence of another important factor, i.e., the incubation time for the luminescent labels and antigens, on the ECL response was studied. As shown in Figure 3, the influence of incubation time of CA199 and SirT1 on the ECL intensity was investigated in a range of 10 to 80 min. An increase in the ECL intensities for CA199 and SirT1 was found as the incubation time increased from 10 to 50 min, after which a seemingly stable state was reached despite with further increase in incubation time.

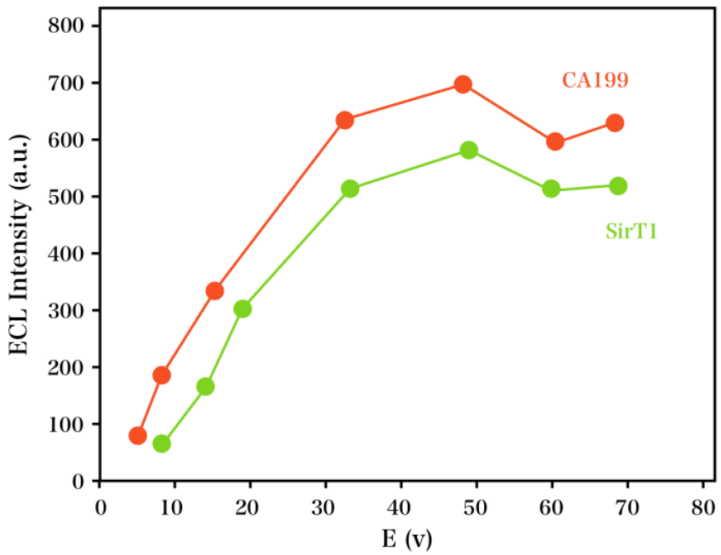

Figure 3. Influence of the incubation time of CA199 and SirT1.

The practical use of our developed immunosensor on the simultaneous determination of CA199 and SirT1 antigens was studied under optimized parameters. As the CA199 and SirT1 concentrations were increased within a range of 0.3 fg/mL - 22 pg/mL, a gradual increase in ECL intensity was found, as displayed in Figure 4A. Figure 4B and C showed the linear regression equations for CA199 and SirT1, respectively. For these two antigens, the LOD was determined to be 0.15 fg/mL (S/N=3). The analytical features of our CA199 and SirT1 biosensor are compared those of previous studies, as shown in Table 1. Compared with other simultaneous determination methods, the fabricated

immunosensor displayed a wider linear range and lower detection limit. These results indicated that the proposed strategy has great potential for practical applications.

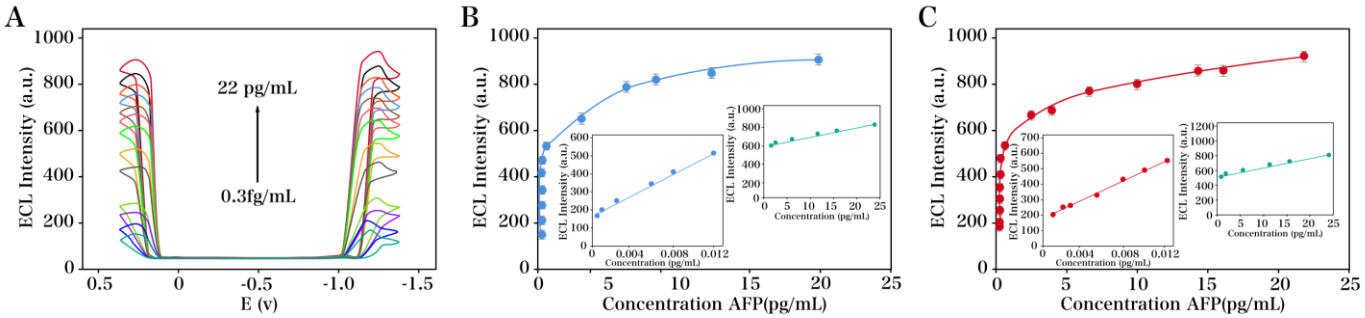

Figure 4. (A) ECL signals of our developed immunosensor in the presence of SirT1 and CA199 at varying concentrations in 0.1 M phosphate buffer (pH 7.4) and 10 mM H_2O_2. (**B**) Calibration pattern for the detection of CA199 (**C**) Calibration pattern for the detection of SirT1.

Table 1. Comparison of the major characteristics of electrochemical sensors used for the detection of SirT1 and CA199.

Electrode	Detection limit of SirT1	Detection limit of CA199	Linear range of SirT1	Linear range of CA199	Reference
Metal ions doped chitosan-poly(acrylic acid)	—	1-150 U/L	—	0.3 U/L	[36]
$Ru(bpy)_3^{2+}$-Silica@Poly-L-lysine-Au	—	0.03-80 U/L	—	0.01 U/L	[37]
AuAg hollow nanocrystals	—	1 to 30 U/mL	—	0.0028 U/mL	[38]
Au@Cu(x)OS yolk-shell	—	0.001 to 12 U/mL	—	0.0005 U/mL	[39]
AuNPs/PDDA-GO	0.029 ng/mL	—	0.1 ng/mL - 100 ng/mL	—	[40]
ECL sensor	0.15 fg/mL	0.15 fg/mL	0.3 fg/mL - 22 pg/mL	0.3 fg/mL - 22 pg/mL	This work

Sensitive and accurate analytical methods need to be developed for the determination of SirT1 [6, 7]. Carbohydrate antigen-199 (CA199) and SirT1 have been confirmed to be related to glioma and pancreatic tumours. Therefore, the simultaneous determination of CA199 and SirT1 in two human serum specimens was carried out with the standard addition method using our developed immunosensor to investigate the applicability and feasibility of this strategy towards the diagnosis of glioma. A comparison of the results obtained using this technique and the standard ELISA method is presented in Table 2. The comparison shows that the results from the two methods are desirably consistent with each other. In addition, CA199 and SirT1 standards spiked into human serum were used to investigate the accuracy of the obtained results. Furthermore, the recovery range was 96.1% to 101.3%, with corresponding RSDs ranging from 3.27% to 4.51%, and 1.78% to 5.02%, for CA199 and

SirT1, respectively. Therefore, our developed ECL immunosensor can potentially be applied to the determination of CA199 and SirT1 in human serum samples. The reproducibility of the biosensor was tested using five proposed biosensors. The prepared electrodes exhibited similar ECL responses and an RSD of 1.75%, which is acceptable for detection.

Table 2. Detection of SirT1 and CA199 in serum specimens using our developed immunosensor and other techniques

Sample	Found	Added	Found (ELISA)	Found (Proposed)	Recovery (%)	RSD (%)
CA199						
1	1.33	2 g/mL	3.52	3.48	104.50	4.51
2	1.08	2 g/mL	3.17	3.21	104.22	3.27
SirT1						
3	1.06	2 g/mL	3.04	3.00	98.04	5.02
4	0.85	2 g/mL	2.74	2.78	97.54	1.78

4. CONCLUSIONS

In this work, the simultaneous determination of CA199 and SirT1 antigens was successfully carried out using an excellent ECL immunoassay, based on a capture apparatus (anti-CA199 (SirT1)) for CA199 (SirT1) via antigen–antibody immunoreactions along with an electrochemiluminophore (ABEI). The results showed that a simultaneous multianalyte immunoassay could be achieved in a single run with our strategy while also eliminating cross-reaction related issues. Therefore, our developed method has considerable potential for the simultaneous detection of tumour markers in biological samples and provides a proof-of-concept for the development of valuable analytical tools for clinical diagnosis of glioma.

References

1. H. Chang and L. Guarente, *Cell*, 153 (2013) 1448.
2. E. Mercken, J. Hu, S. Krzysik-Walker, M. Wei, Y. Li, M. McBurney, R. Cabo and V. Longo, *Aging Cell*, 13 (2014) 193.
3. H. Jeong, D.. Cohen, L. Cui, A. Supinski, J. Savas, J. Mazzulli, J. Yates Iii, L. Bordone, L. Guarente and D. Krainc, *Nature Medicine*, 18 (2012) 159.
4. T. Mimura, Y. Kaji, H. Noma, H. Funatsu and S. Okamoto, *Experimental Eye Research*, 116 (2013) 17.
5. B. Rogina and S. Helfand, *Proceedings of the National Academy of Sciences of the United States of America*, 101 (2004) 15998.
6. P. Fabrizio, C. Gattazzo, L. Battistella, M. Wei, C. Cheng, K. McGrew and V. Longo, *Cell*, 123 (2005) 655.
7. M. Kaeberlein, K. Kirkland, S. Fields and B. Kennedy, *PLoS Biology*, 2 (2004) e296.
8. G. Lai, J. Wu, C. Leng, H. Ju and F. Yan, *Biosensors and Bioelectronics*, 26 (2011) 3782.

9. Y. Cheng, T. Rees and J. Wright, *Clinical and Translational Medicine*, 3 (2014) 3.
10. T. Zheng, N. Pierre-Pierre, X. Yan, Q. Huo, A. Almodovar, F. Valerio, I. Rivera-Ramirez, E. Griffith, D. Decker and S. Chen, *ACS Applied Materials & Interfaces*, 7 (2015) 6819.
11. Q. Zhao, R. Duan, J. Yuan, Y. Quan, H. Yang and M. Xi, *International Journal of Nanomedicine*, 9 (2014) 1097.
12. M. Vendrell, K. Maiti, K. Dhaliwal and Y. Chang, *Trends in Biotechnology*, 31 (2013) 249.
13. R. Devi, M. Doble and R. Verma, *Biosensors and Bioelectronics*, 68 (2015) 688.
14. Z. Tian, J. Li, Z. Zhang, W. Gao, X. Zhou and Y. Qu, *Biomaterials*, 59 (2015) 116.
15. M. Iranifam, *TrAC Trends in Analytical Chemistry*, 59 (2014) 156.
16. I. Al-Ogaidi, H. Gou, Z.P. Aguilar, S. Guo, A. Melconian, A. Al-Kazaz, F. Meng and N. Wu, *Chemical Communications*, 50 (2014) 1344.
17. A. Chinen, C. Guan, J. Ferrer, S. Barnaby, T. Merkel and C. Mirkin, *Chemical Reviews*, 115 (2015) 10530.
18. B. Kavosi, A. Salimi, R. Hallaj and F. Moradi, *Biosensors and Bioelectronics*, 74 (2015) 915.
19. S. Hettiarachchi, B. Prasai and R. McCarley, *Journal of the American Chemical Society*, 136 (2014) 7575.
20. K. Shi, B. Dou, C. Yang, Y. Chai, R. Yuan and Y. Xiang, *Analytical Chemistry*, 87 (2015) 8578.
21. Z. Zhao, Y. Yang, Y. Zeng and M. He, *Lab on a Chip*, 16 (2016) 489.
22. D. Taller, K. Richards, Z. Slouka, S. Senapati, R. Hill, D. Go and H. Chang, *Lab on a Chip*, 15 (2015) 1656.
23. K. Haraguchi, S. Sato, M. Habu, N. Yada, M. Hayakawa, O. Takahashi, I. Yoshioka, K. Matsuo, K. Tominaga and S. Takenaka, *Electroanalysis*, 29 (2017) 1596.
24. J. Raj, G. Herzog, M. Manning, C. Volcke, B.D. MacCraith, S. Ballantyne, M. Thompson and D. Arrigan, *Biosensors and Bioelectronics*, 24 (2009) 2654.
25. M. Mohammed and M. Desmulliez, *Biosensors and Bioelectronics*, 61 (2014) 478.
26. J. Wu, G. Huang, H. Li, S. Wu, Y. Liu and J. Zheng, *Polymer*, 54 (2013) 1930.
27. N. Frey, S. Peng, K. Cheng and S. Sun, *Chemical Society Reviews*, 38 (2009) 2532.
28. H. Teymourian, A. Salimi and S. Khezrian, *Biosensors and Bioelectronics*, 49 (2013) 1.
29. M. Yang, C. Liu, K. Qian, P. He and Y. Fang, *Analyst*, 127 (2002) 1267.
30. F. Sun, F. Chen, W. Fei, L. Sun and Y. Wu, *Sensors and Actuators B: Chemical*, 166 (2012) 702.
31. F. Nie, K. Luo, X. Zheng, J. Zheng and Z. Song, *Sensors & Actuators B Chemical*, 218 (2015) 152.
32. G. Gui, Y. Zhuo, Y. Chai, Y. Xiang and R. Yuan, *Biosensors & Bioelectronics*, 70 (2015) 221.
33. L. Zhou, J. Wang, D. Li and Y. Li, *Food Chemistry*, 162 (2014) 34.
34. R. Chand, D. Han, S. Neethirajan and Y. Kim, *Sensors and Actuators B: Chemical*, 248 (2017) 973.
35. M. Huang, H. Li, H. He, X. Zhang and S. Wang, *Analytical Methods*, 8 (2016) 7413.
36. Q. Rong, F. Feng and Z. Ma, *Biosensors & Bioelectronics*, 75 (2016) 148.
37. X. Feng, N. Gan, J. Zhou, T. Li, Y. Cao, F. Hu, H. Yu and Q. Jiang, *Electrochimica Acta*, 139 (2014) 127.
38. R. Wang, J. Feng, W. Liu, L. Jiang and A. Wang, *Biosensors & Bioelectronics*, 96 (2017) 152.
39. A. Guo, Y. Li, W. Cao, X. Meng, D. Wu, Q. Wei and B. Du, *Biosensors & Bioelectronics*, 63 (2015) 39.
40. W. Bi, D. Lu, Y. Fu, Q. Huang, Z. Xu and W. Zhang, *Chemical Journal of Chinese Universities*, 34 (2013) 1612